



UNIVERSITAT DE BARCELONA



# The search for massive protostars

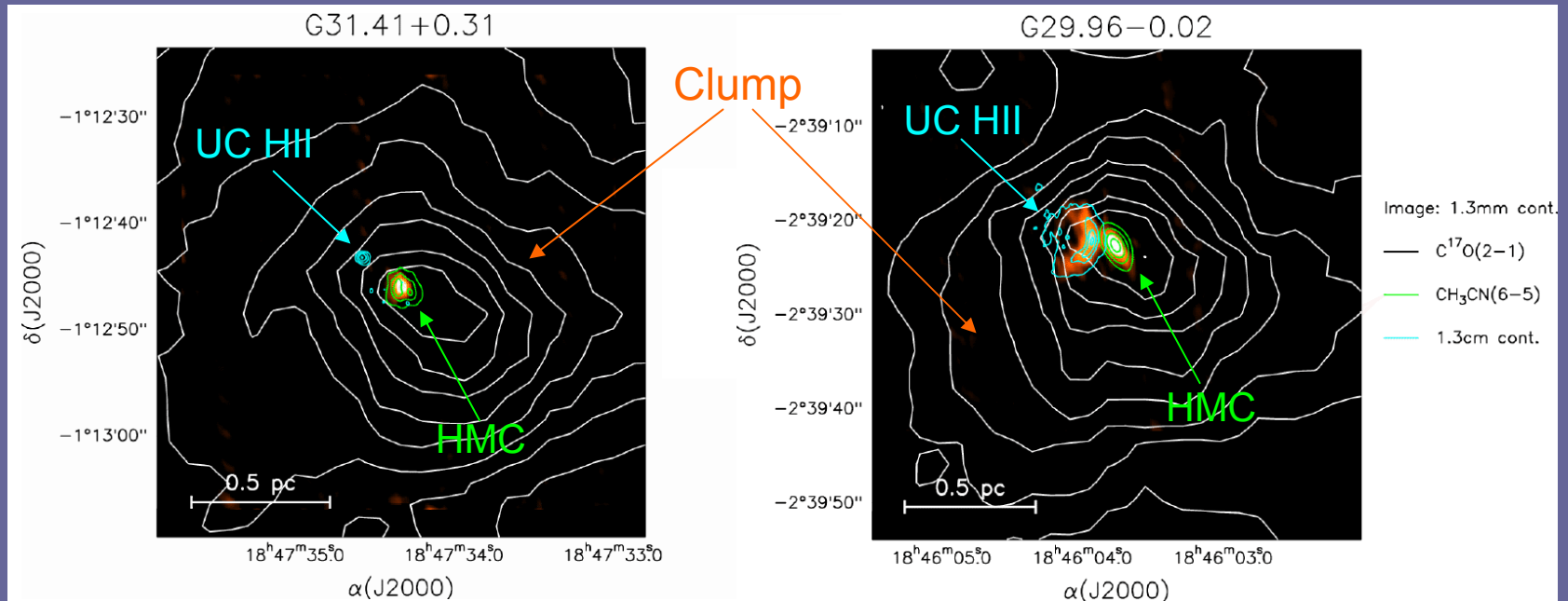
**Maite Beltrán**

**Departament d'Astronomia i Meteorologia  
Universitat de Barcelona**

Riccardo Cesaroni, Claudio Codella, Leonardo Testi, Luca Olmi, Luca Moscadelli (Arcetri), Roberto Neri (IRAM), Ray Furuya (NAOJ)

# Sites of massive star formation

- High-mass star-forming regions host luminous FIR point sources, UC HII regions, and newly formed OB stars embedded in rich hot molecular cores that can be studied using a variety of tracers.

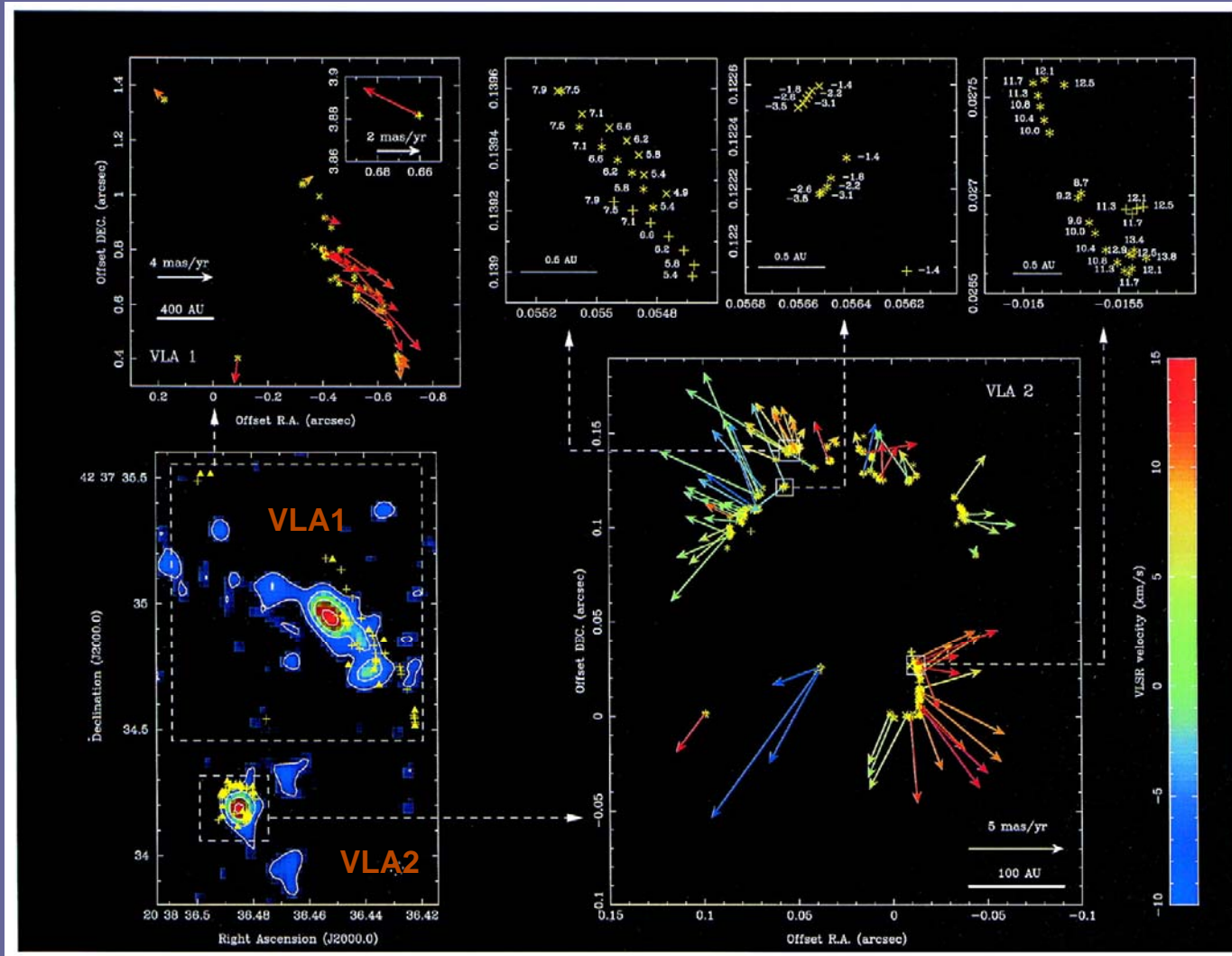


# Sites of massive star formation

- High-mass star-forming clouds host luminous FIR point sources, UC HII regions, and newly formed OB stars embedded in rich hot molecular cores than can be studied using a variety of tracers.
- In particular,  $\text{H}_2\text{O}$ ,  $\text{CH}_3\text{OH}$ , and OH masers are often observed close to these typical signposts of massive stars.

# Sites of massive star formation

- 3 epoch water maser VLBA towards W75N-VLA1 and VLA2

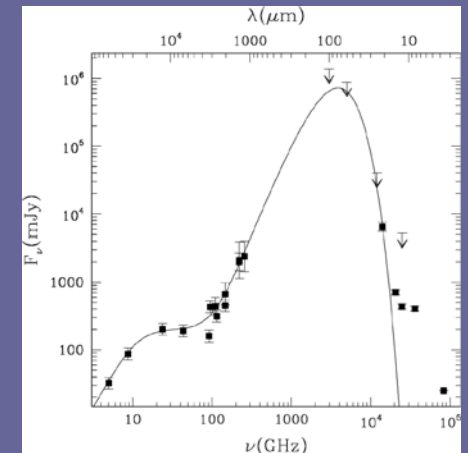
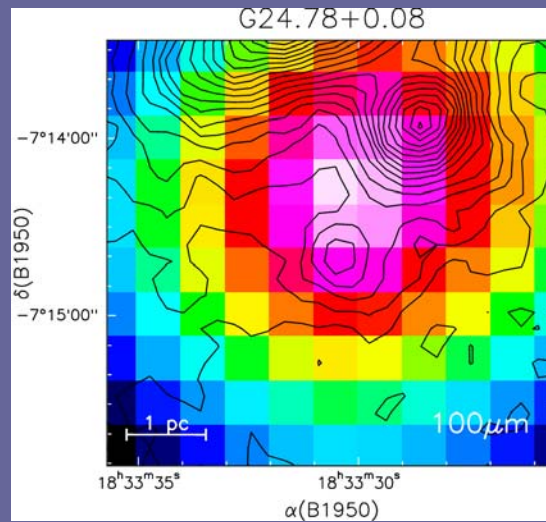
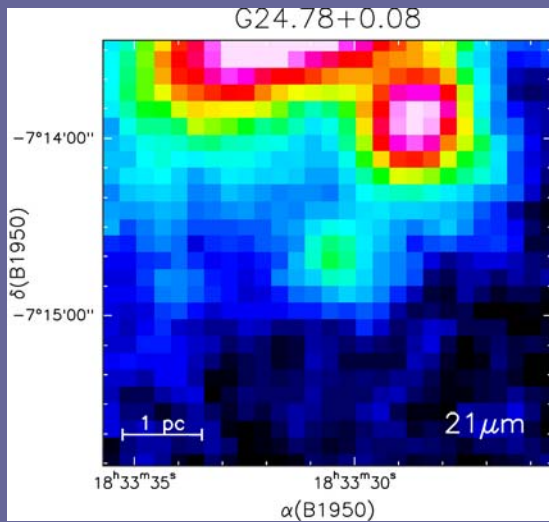
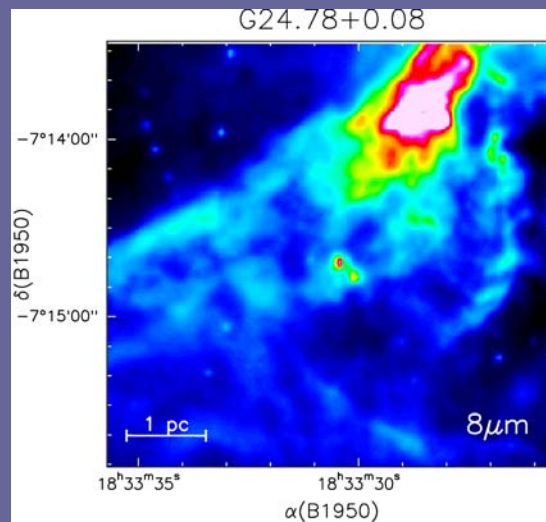
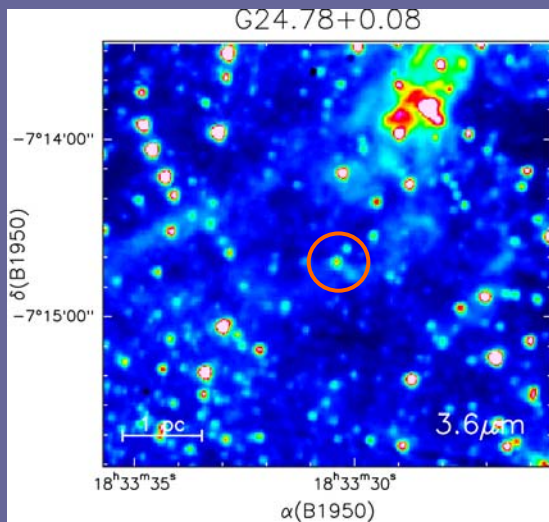


Torrelles et al. (2003)

# Sites of massive star formation

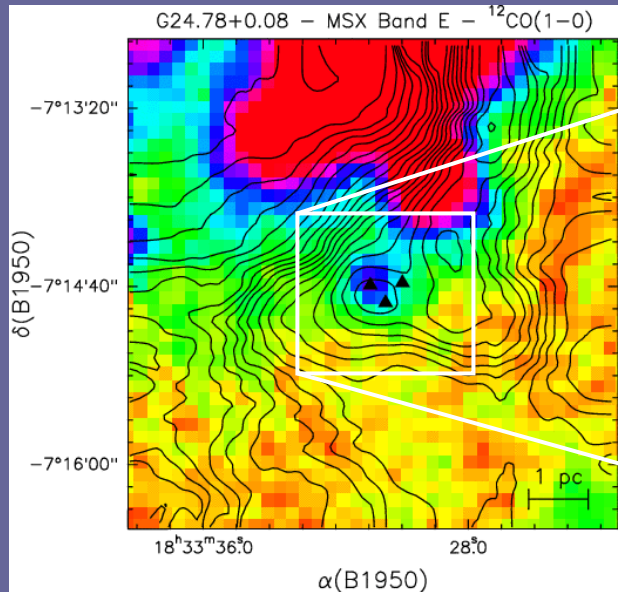
- High-mass star-forming clouds host luminous FIR point sources, UC HII regions, and newly formed OB stars embedded in rich hot molecular cores than can be studied using a variety of tracers.
- In particular, H<sub>2</sub>O, CH<sub>3</sub>OH and OH masers are often observed close to these typical signposts of massive stars.
- Codella et al. (1997) carried out a NH<sub>3</sub> survey with the Medicina antenna towards a sample of H<sub>2</sub>O and OH maser sources associated with infrared sources to assess the presence of molecular cores associated with the maser spots.
- The MSFR G24.78+0.08 was among the strongest NH<sub>3</sub> emitters and the clump was thoroughly observed in other tracers and with higher angular resolution.

# G24.78+0.08: the clump

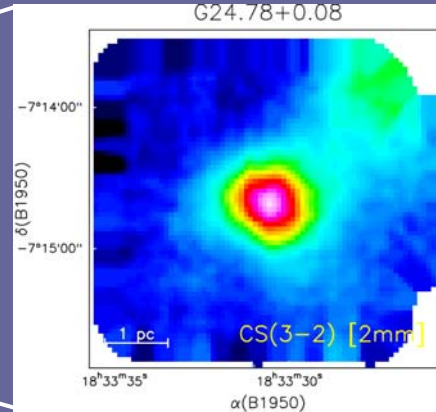


- G24.78 is located at a distance of 7.7 kpc
- $L_{\text{IRAS}} = 7 \times 10^5 L_{\odot}$

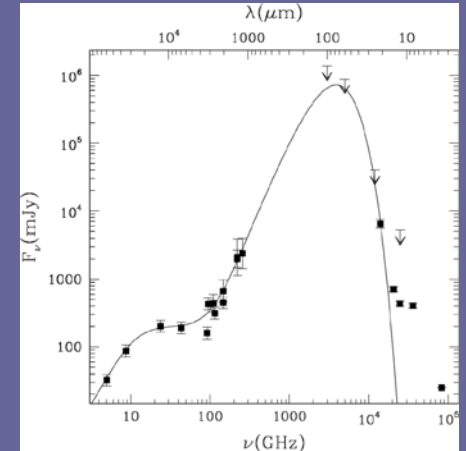
# G24.78+0.08: the clump



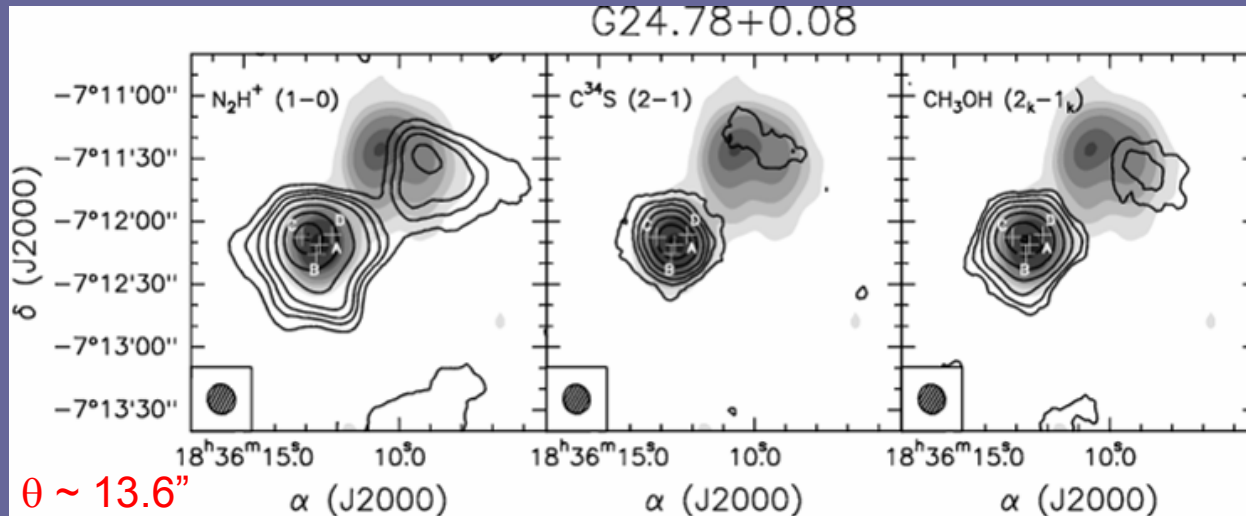
IRAM 30-m



Cesaroni et al. (2003)



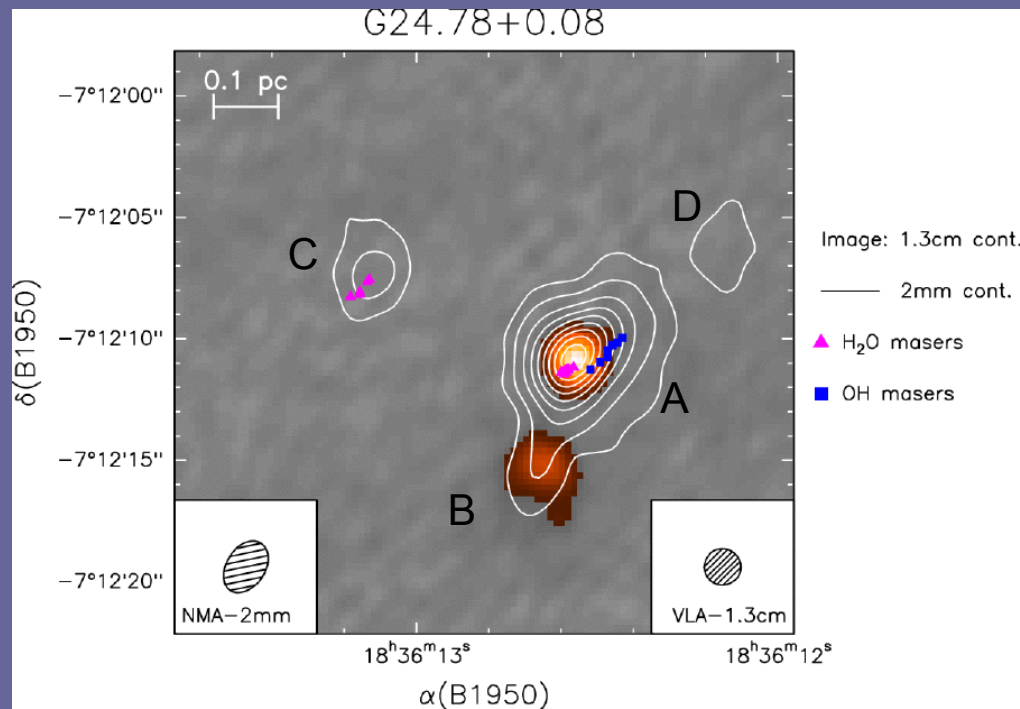
BIMA interf.



Beltrán et al. (2005)

# G24.78+0.08: the hot core

- The clump is hosting a cluster of massive YSOs in different evolutionary stage:



- All cores associated with mm continuum emission
- two of them (A and C) associated with maser emission
- two of them (A and B) associated with UC HII regions

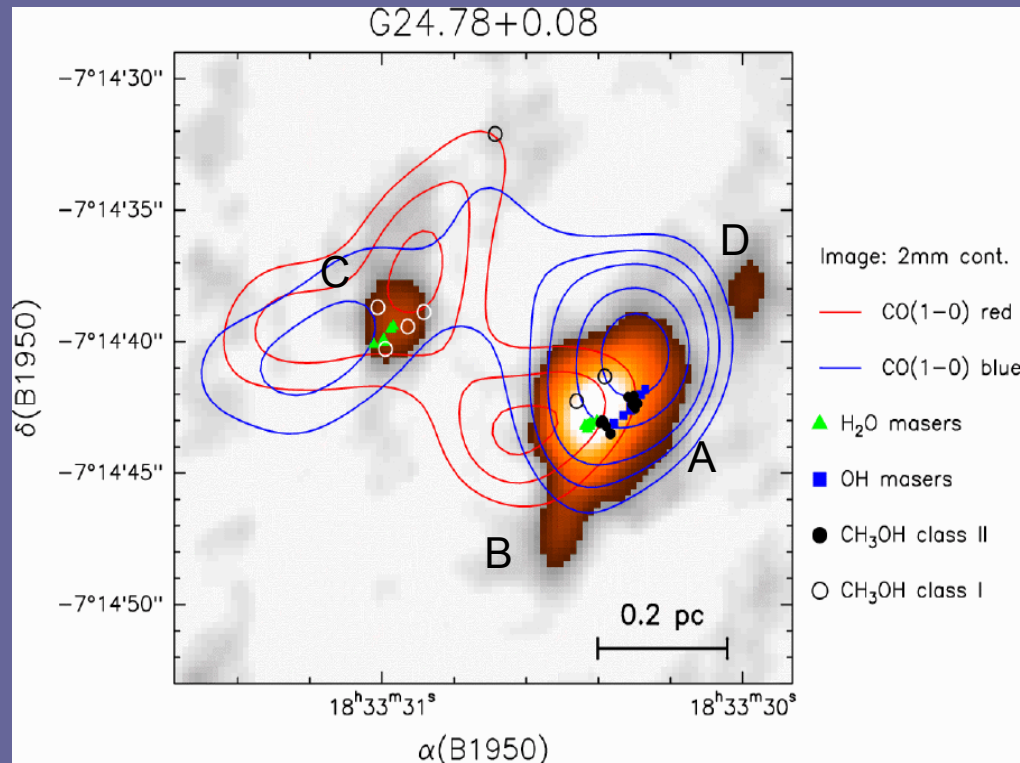
Codella et al. (1997)

Furuya et al. (2002)



# G24.78+0.08: the hot core

- The clump is hosting a cluster of massive YSOs in different evolutionary stage:

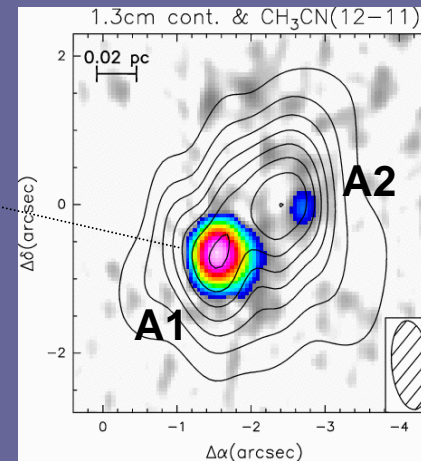
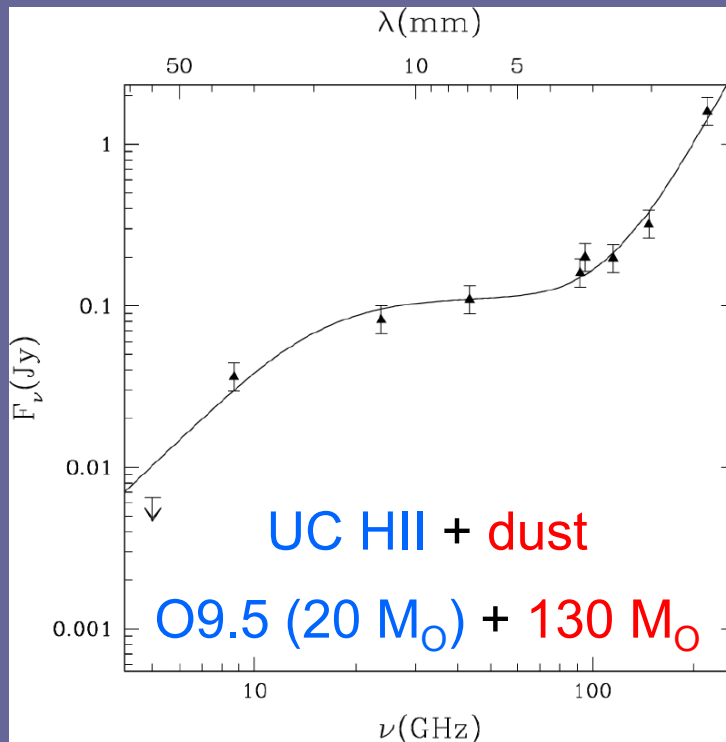


Furuya et al. (2002)

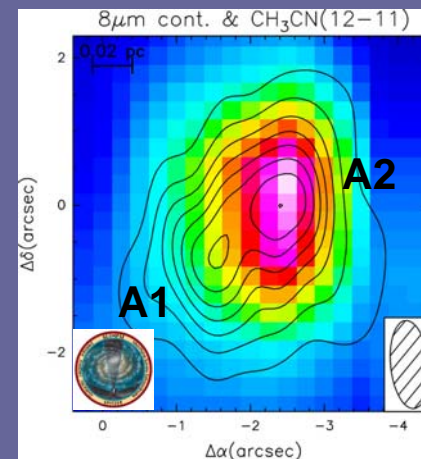
- All cores associated with mm continuum emission
- two of them (A and C) associated with maser emission
- two of them (A and B) associated with UC HII regions
- two of them (A and C) powering molecular outflows

# G24.78+0.08: the cores A1 and A2

- High-angular resolution mm continuum and CH<sub>3</sub>CN PdBI observations have resolved the core A into two separate cores, named A1 and A2, probably in different evolutionary stage.



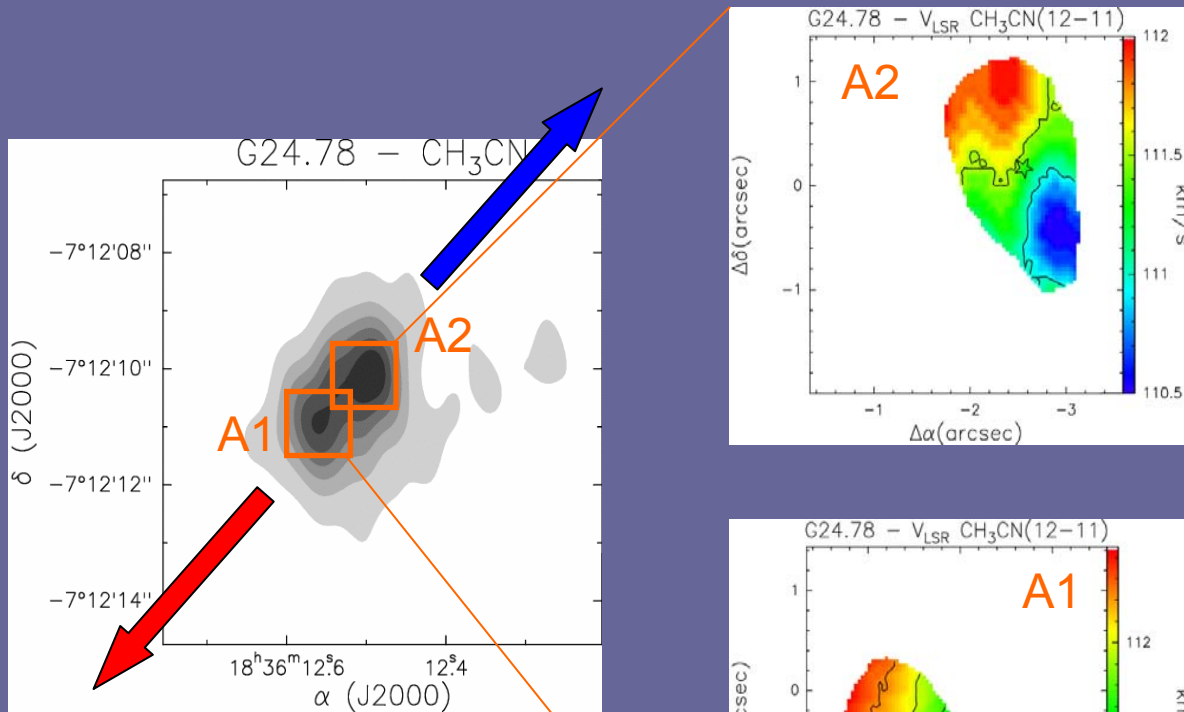
PdBI + VLA



PdBI + Spitzer

# G24.78+0.08 A1 and A2: rotation

- To search for velocity gradients in the cores, we have fitted simultaneously the multiple K-components of the different rotational transitions of CH<sub>3</sub>CN(12-11)



Beltrán et al. (2004)

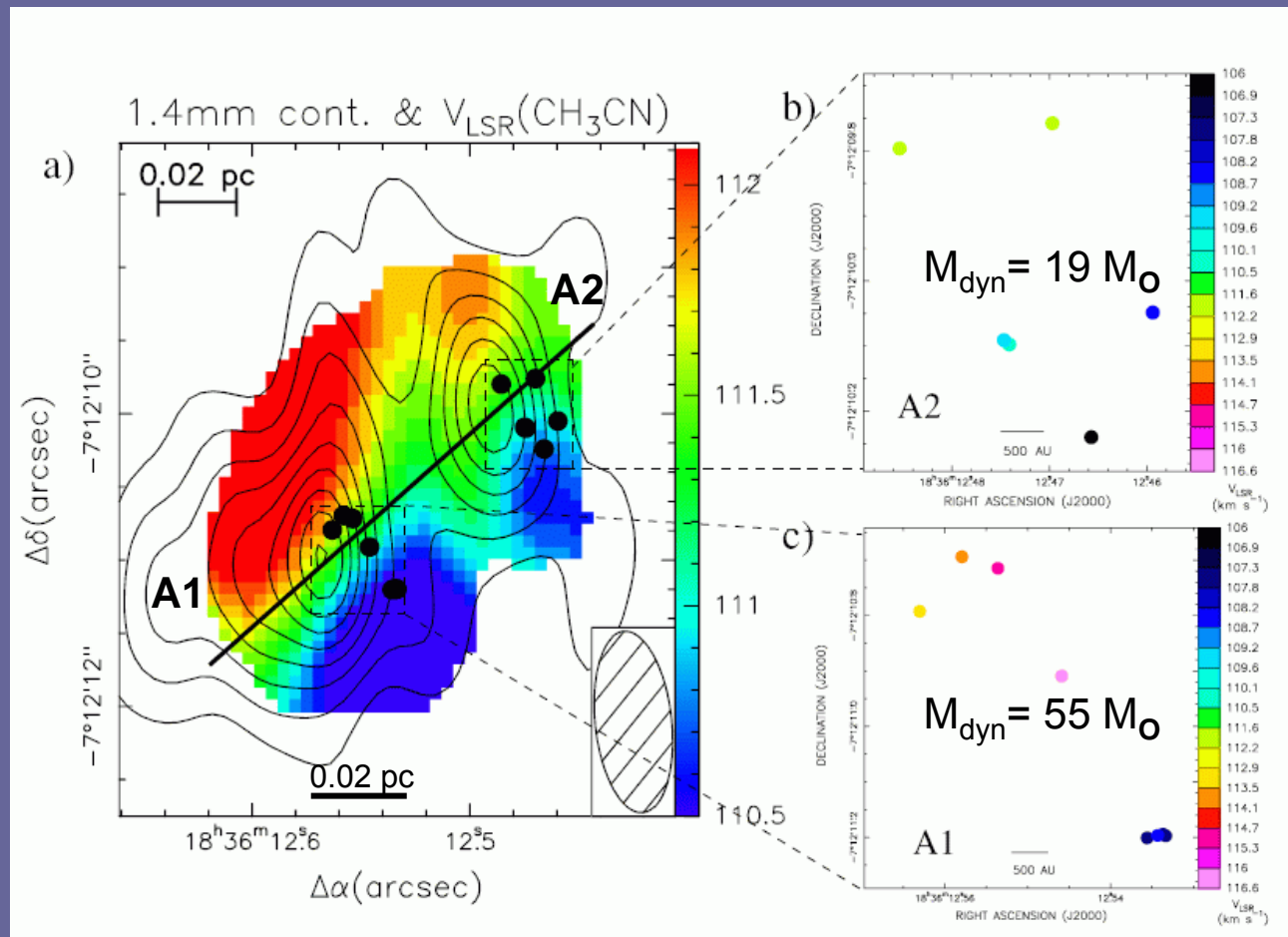
- Parameters of the toroids

$$\begin{aligned}
 R &= 4000 \text{ AU} \\
 M_{\text{gas}} &= 80 M_{\odot} \\
 M_{\text{dyn}} &= 4 M_{\odot} \\
 V_{\text{rot}} &= 0.75 \text{ km/s} \\
 \dot{M}_{\text{accr}} &= 8 \times 10^{-3} M_{\odot}/\text{yr} \\
 t_{\text{accr}} &= 1 \times 10^4 \text{ yr}
 \end{aligned}$$

$$\begin{aligned}
 R &= 4000 \text{ AU} \\
 M_{\text{gas}} &= 130 M_{\odot} \\
 M_{\text{dyn}} &= 23 M_{\odot} \\
 V_{\text{rot}} &= 1.50 \text{ km/s} \\
 \dot{M}_{\text{accr}} &= 2 \times 10^{-2} M_{\odot}/\text{yr} \\
 \dot{M}_{\text{out}} &= 5 \times 10^{-4} M_{\odot}/\text{yr} \\
 t_{\text{accr}} &= 7 \times 10^3 \text{ yr} \\
 t_{\text{out}} &= 2 \times 10^4 \text{ yr}
 \end{aligned}$$

# G24.78+0.08 A1 and A2: rotation

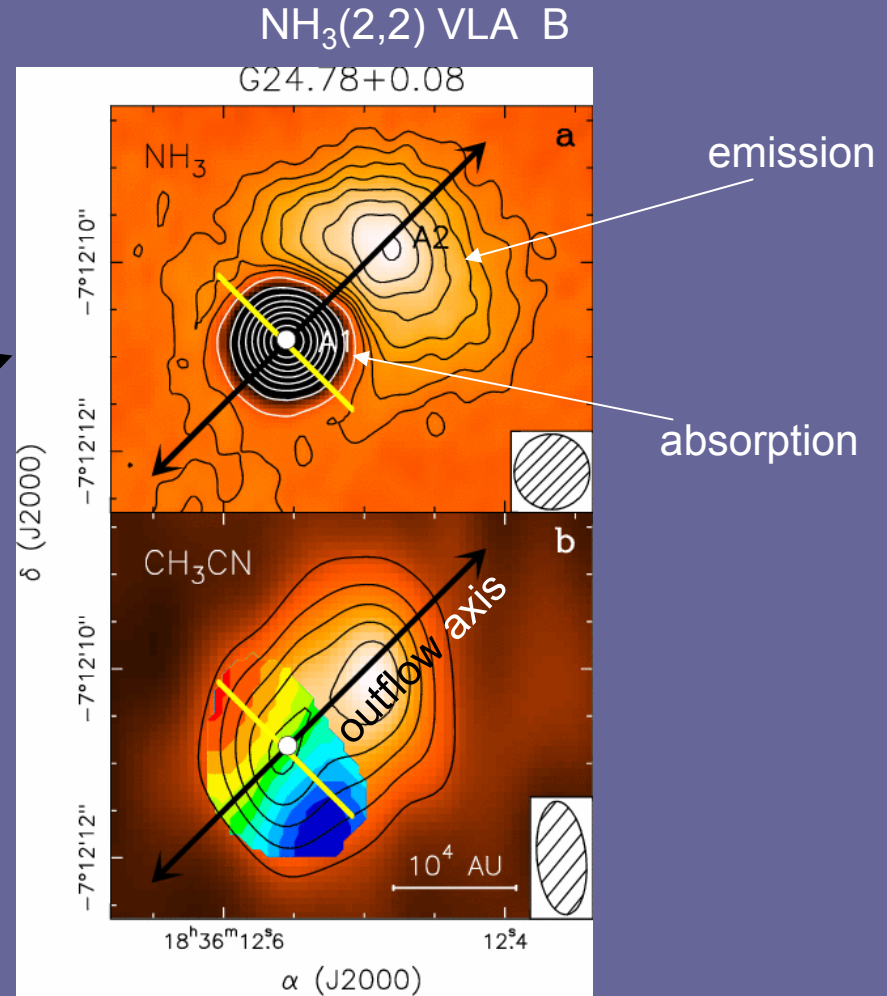
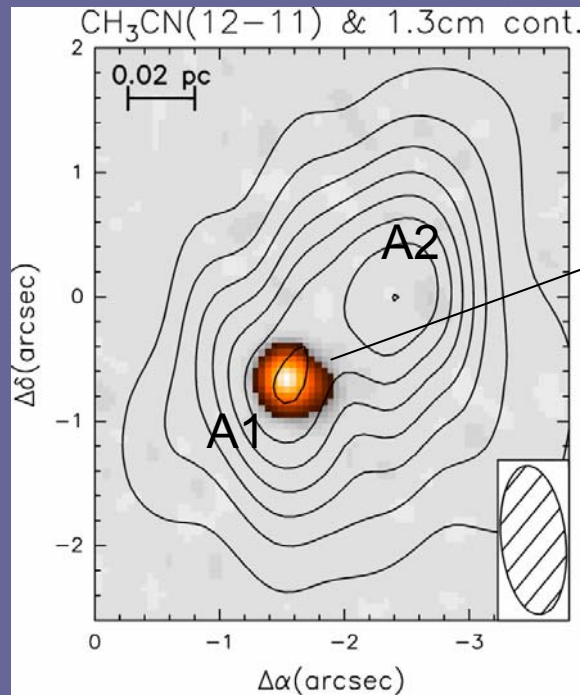
- EVN methanol maser emission observations have revealed two groups of masers associated with cores A1 and A2, aligned perpendicular to the direction of the bipolar outflow and with a velocity gradient consistent with the CH<sub>3</sub>CN one.



Moscadelli et al (2007)

# G24.78+0.08 A1: infall

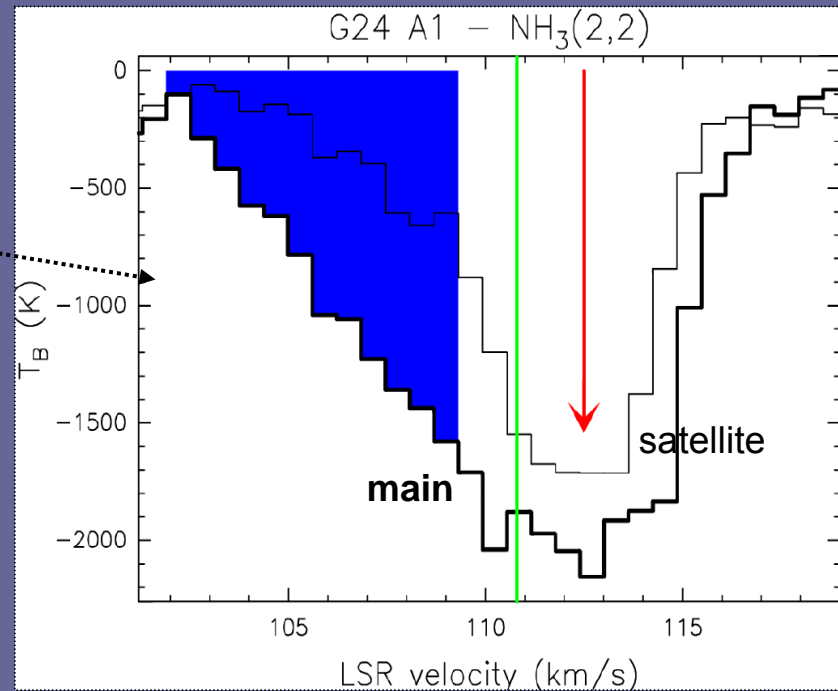
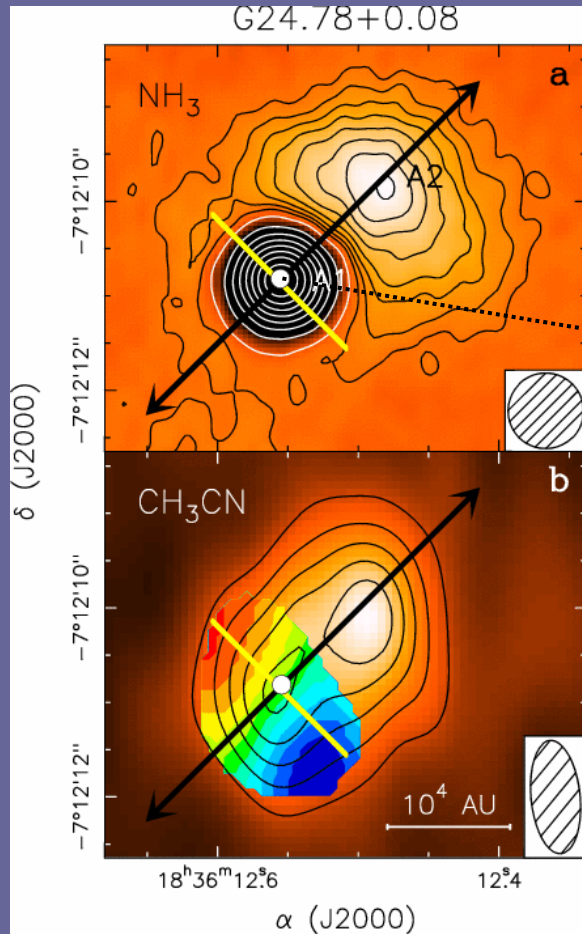
- The HC III associated with G24 A1 is very bright at cm  $\lambda$ 's ( $>2000$  K), it is easy to observe the colder molecular gas ( $\sim 100$  K) in absorption against it.



Beltrán et al. (2006)

# G24.78+0.08 A1: infall

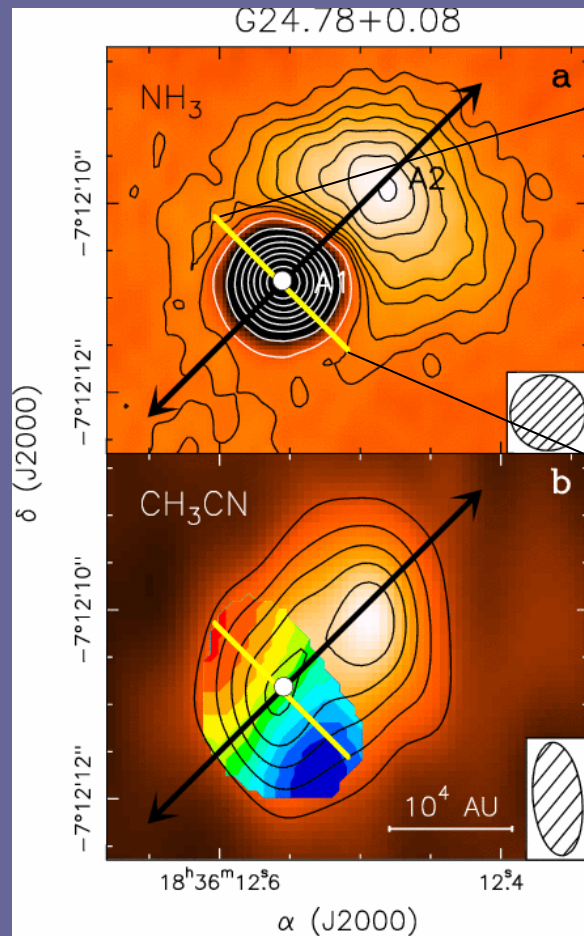
- Towards the HC III, the satellite absorption is strongly biased towards positive velocities; the peak of the satellite absorption is red-shifted  $\sim 2$  km/s.



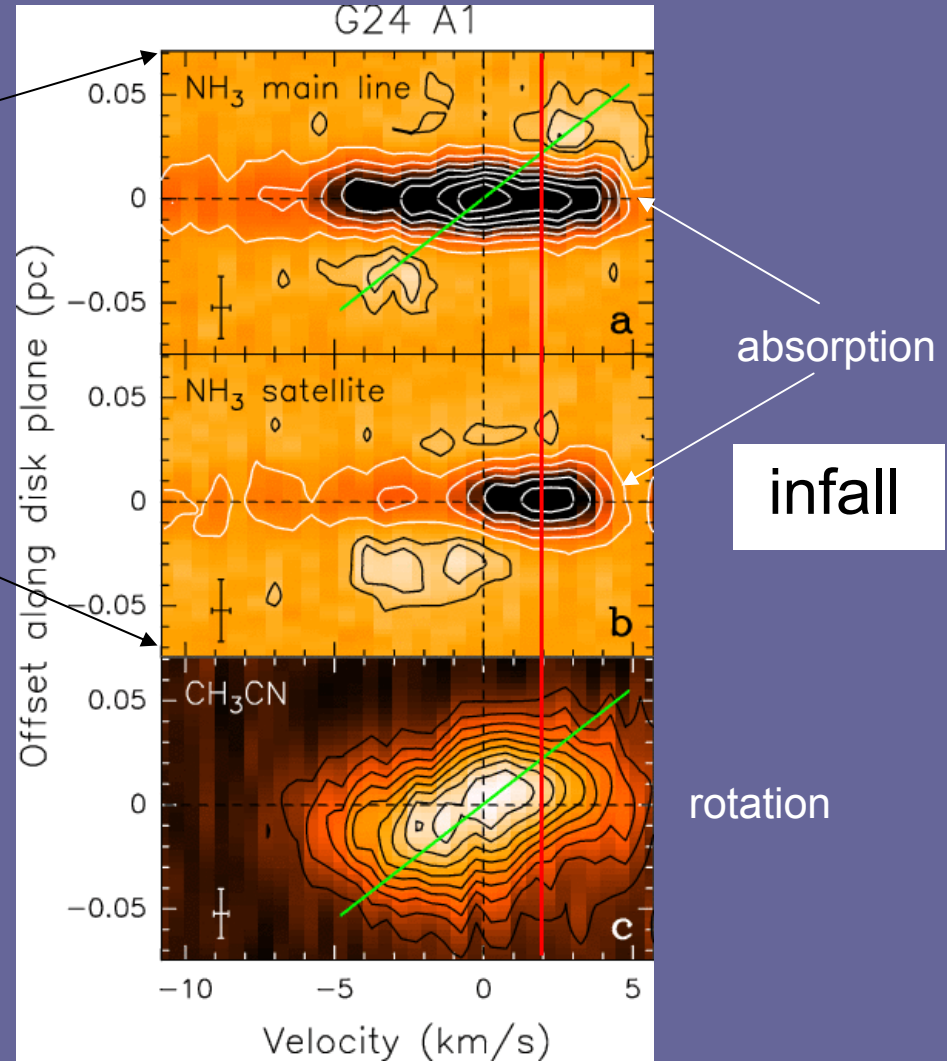
Beltrán et al. (2006)

# G24.78+0.08 A1: infall

- Towards the HC III, the satellite absorption is strongly biased towards positive velocities; the peak of the satellite absorption is red-shifted  $\sim 2$  km/s.



Beltrán et al. (2006)



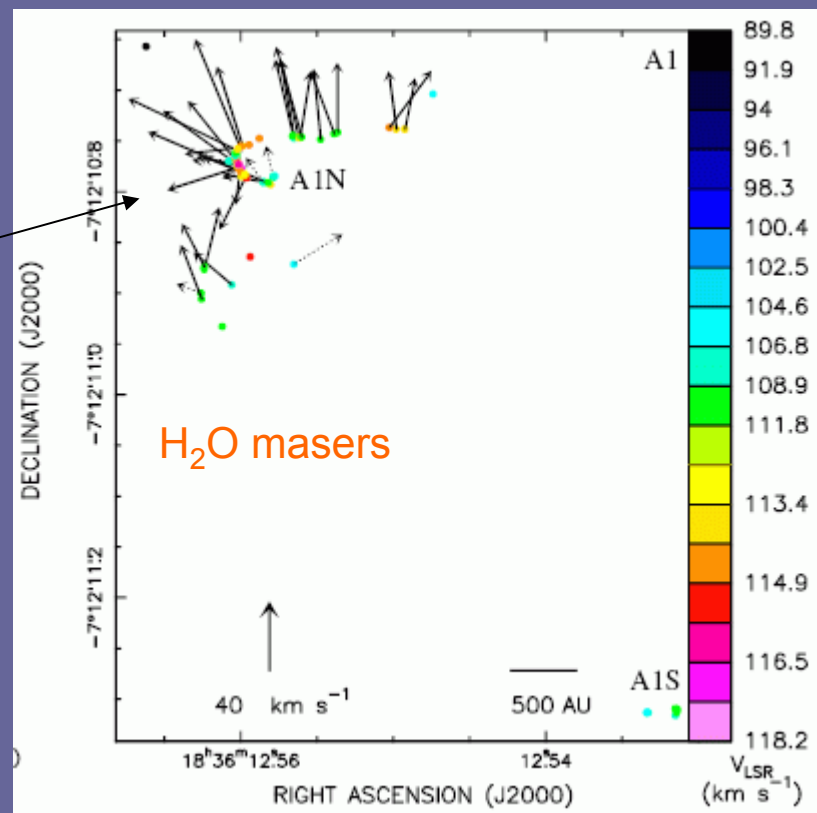
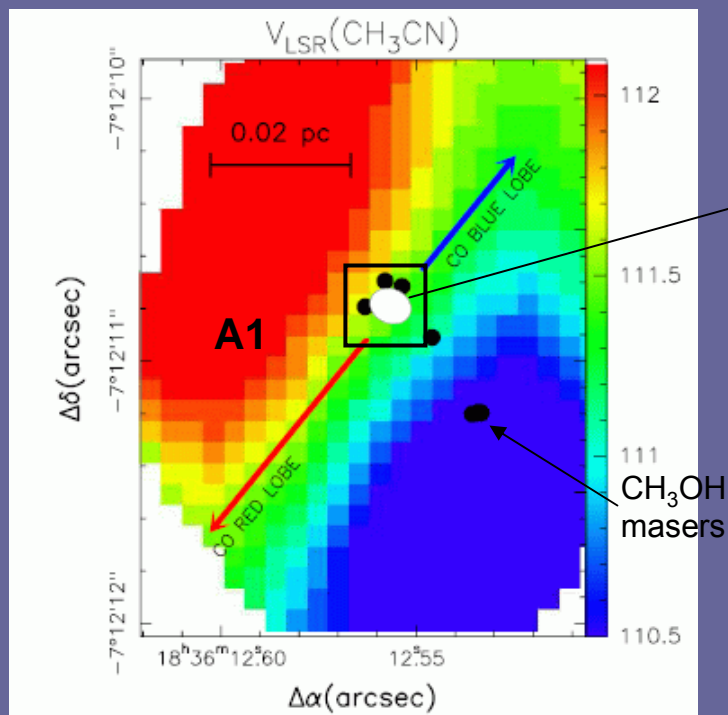
# G24.78+0.08 A1: infall

- Towards the HC III, the satellite absorption is strongly biased towards positive velocities; the peak of the satellite absorption is red-shifted  $\sim 2$  km/s.
- This indicates that the toroid is not only rotating but also accreting onto the central object.
- From  $N_{\text{H}_2} = 6 \times 10^{23} - 6 \times 10^{24} \text{ cm}^{-2}$ , and the infall velocity  $v_{\text{infall}} = 2$  km/s, assuming free-fall, one obtains the mass accretion rate onto a solid angle  $\Omega$ :  
$$\dot{M}_{\text{accr}} = \frac{\Omega}{4\pi} [(4 \times 10^{-4}) - 10^{-2}] M_{\odot} \text{ yr}^{-1}$$
- The radius at which is measured is estimated to be  $0.1'' < R < 1''$  ( $0.0037 < R < 0.037$  pc)
- $(dM/dt)_{\text{infall}}$  is much larger than the critical rate above which formation of an HII region is inhibited if the accretion is spherical ( $\Omega=4\pi$ ),  $(dM/dt)_{\text{inh}} \approx 8 \times 10^{-6} M_{\odot} \text{ yr}^{-1}$ . The fact that the HII exists can be explained only if the accretion is not spherically symmetric ( $\Omega < 4\pi$ )



# G24.78+0.08 A1: expansion?

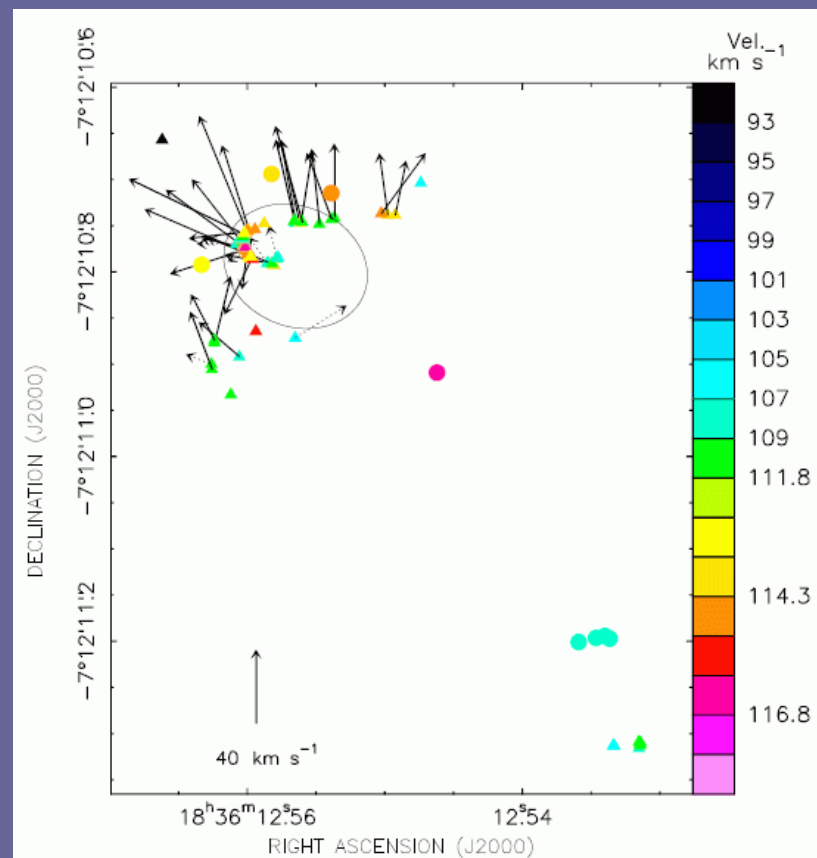
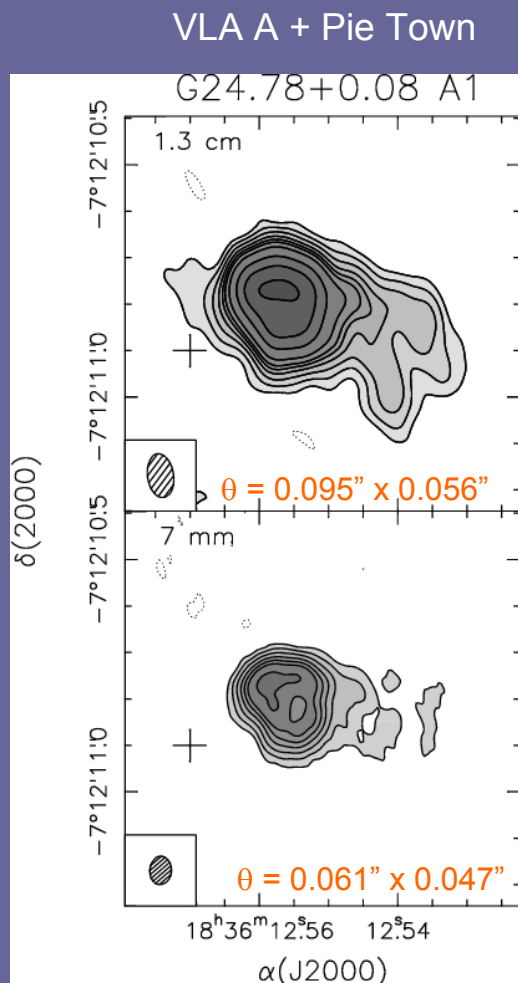
- Recent multi-epoch 22 GHz water maser VLBA observations have clearly shown evidences for expanding motions perpendicular to the outflow main axis (along the plane of the rotating and infalling toroid).



Moscadelli et al. (2007)

# G24.78+0.08 A1: expansion?

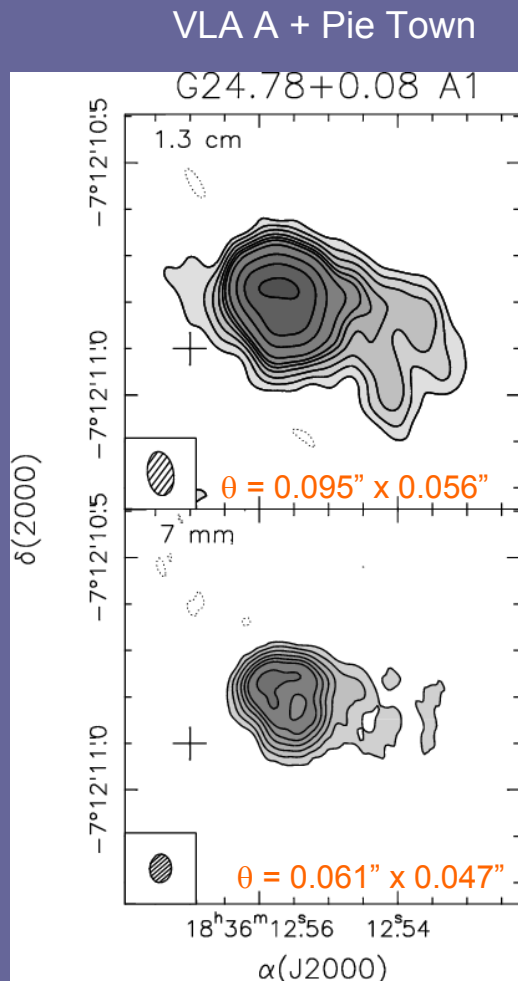
- The HC III region has a ring-shaped structure with an outer radius of  $\sim 550$ - $580$  AU with the  $\text{H}_2\text{O}$  maser features distributed along the border of the ionized gas.



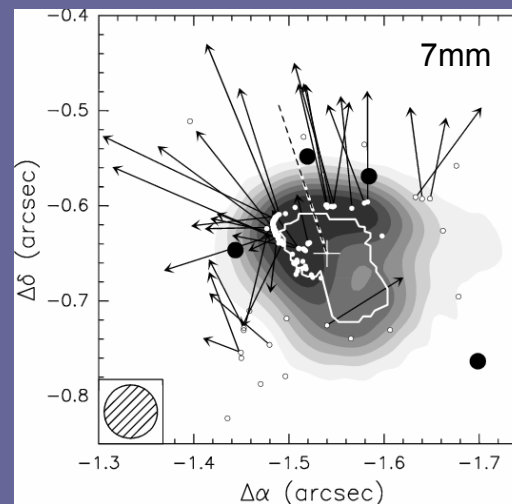
- The position and geometry of the continuum source suggest that the motion of the water masers can be driven by the expansion of the ionized gas

# G24.78+0.08 A1: expansion?

- The HC III region has a ring-shaped structure with an outer radius of  $\sim 550$ - $580$  AU with the  $\text{H}_2\text{O}$  maser features distributed along the border of the ionized gas.



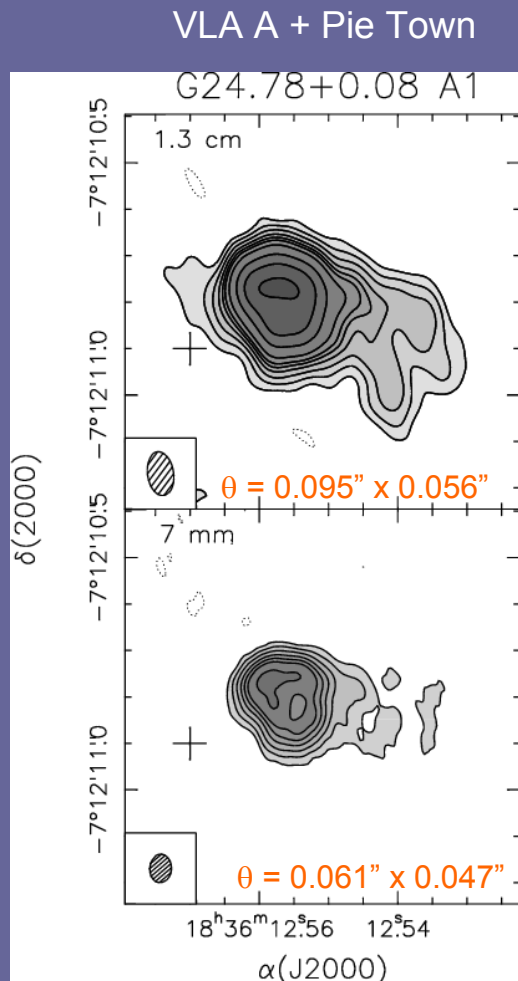
Beltrán et al. (2007)



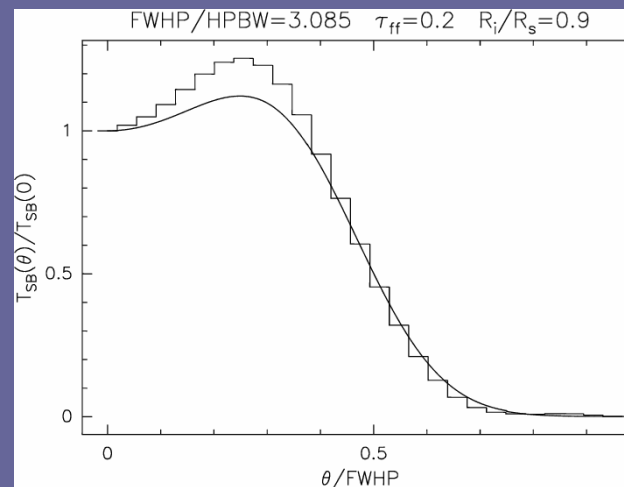
- The profiles of the emission obtained at different angles by taking slices passing through the barycenter of the HC III show two peaks, as one would expect in the case of an emission ring.

# G24.78+0.08 A1: expansion?

- The HC III region has a ring-shaped structure with an outer radius of  $\sim 550$ - $580$  AU with the  $\text{H}_2\text{O}$  maser features distributed along the border of the ionized gas.



Beltrán et al. (2007)



- The fit to the normalized temperature profile along a cut passing through the barycenter at 7mm and the peak of emission.
- For an optical depth of 0.2 and  $T_e = 10^4$  K, the best fit is obtained when  $R_i/R_o \sim 0.9 \rightarrow$  very thin shell  $\rightarrow$  radius of the shell  $\sim 590$  AU.

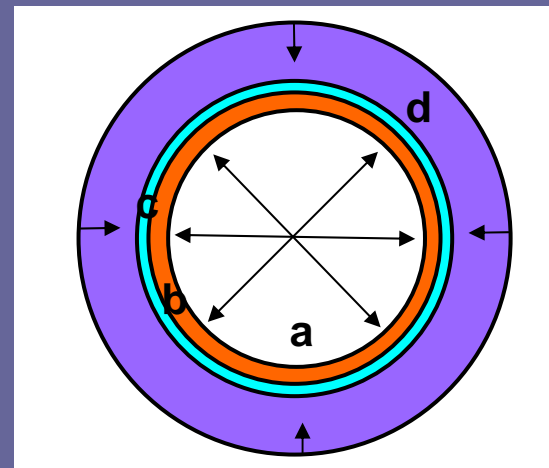
# G24.78+0.08 A1: expansion

- The water masers appear to be tracing expansion, which suggests that the HC III is expanding. Because of the high velocities ( $\sim 40$  km/s), the expansion cannot be led by the thermal pressure of the ionized gas (e.g. Deprea et al. 1995,  $v \sim 10$  km/s). It must be an additional mechanism driving the expansion.
- According to Shull (1980), the HII region expansion might be driven by a powerful stellar wind.

I. Initial phase of free expansion at the wind velocity, when the wind sweeps up its own mass in interstellar matter

II. Four-zone structure, in which a thin, dense ionized shell that contains most of the swept up material is created:

- a) free-flowing wind
- b) thin region of hot shocked wind material
- c) thin, dense shell of swept-up of HMC material
- d) accreting HMC

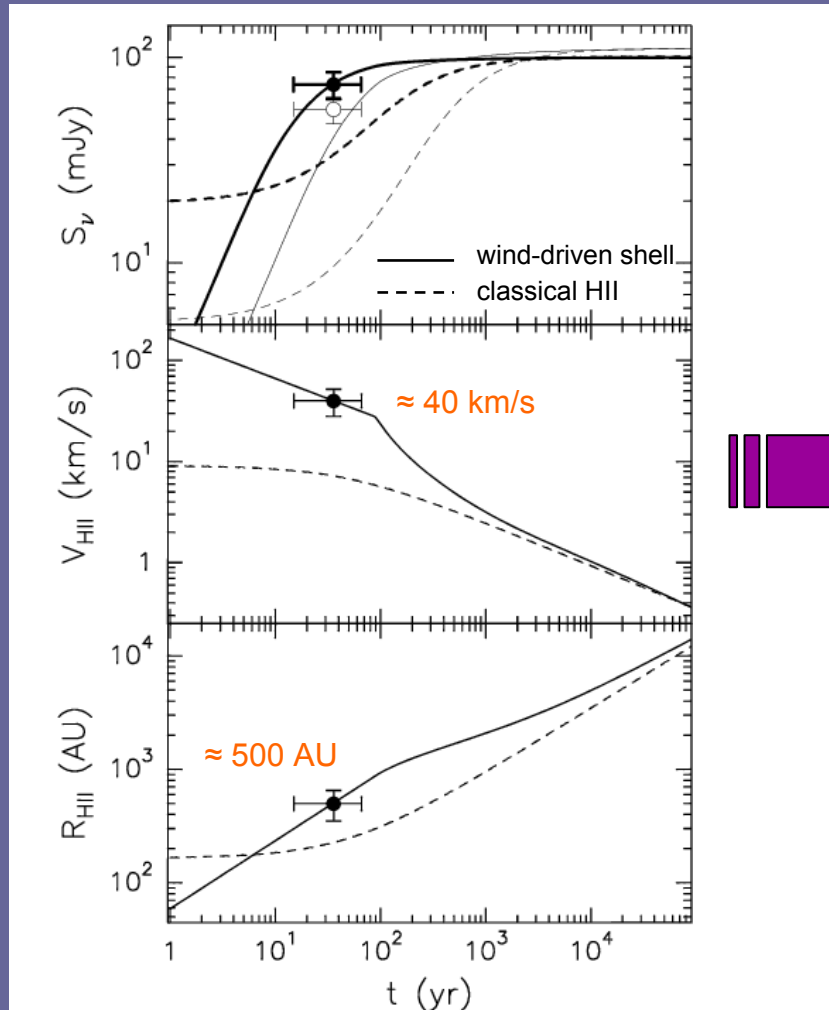


(see e.g. González-Avilés et al. 2005)

- **Two phases can be identified:** a pressure-driven expansion followed by a momentum-driven expansion (after a critical time that depends on the wind mechanical luminosity and density of the surrounding environment).

# G24.78+0.08 A1: expansion

- For a wind mechanical luminosity ( $10^{36}$  ergs) and density ( $10^7$  cm $^{-3}$ ),  $R_{\text{HII}}$  and  $V_{\text{HII}}$  of the expanding shell can be expressed as a function of time (Shull 1980).  $V_{\text{wind}}=2000$  km/s for O9.5

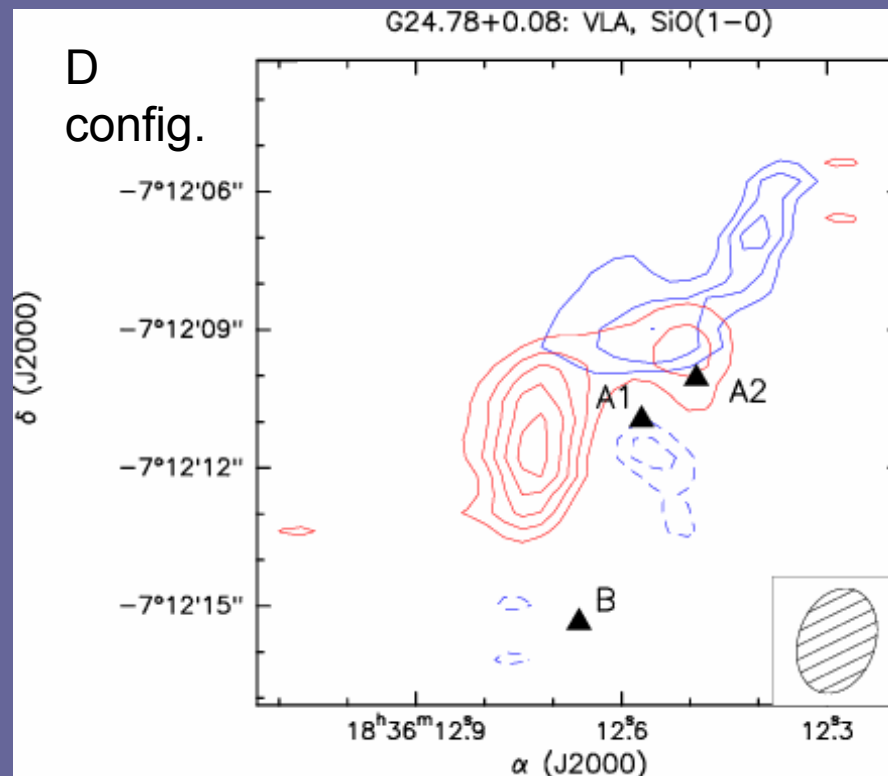


Beltrán et al. (2007)

The solution of the wind-driven expansion that reproduces the observed shell parameters predicts a shell age of 21-66 yr !

# G24.78+0.08 A1: rotation or expansion?

- Is the velocity gradient observed in the thermal  $\text{CH}_3\text{CN}$  (12-11) line as well in the  $\text{CH}_3\text{OH}$  maser emission due to expansion rather than rotation? Is there a collimated, compact bipolar outflow, perpendicular to the outflow seen on a larger scale in the  $\text{CO}(1-0)$  line?



# G24.78+0.08 A1: the global view

- G24.78+0.08 A1 is a  $20 M_{\odot}$  where for the first time, the simultaneous presence of the “ingredients” expected in a typical star formation scenario has been detected: rotation, outflow and infall. The large accretion rate and the existence of an HC HII region at the center of the rotating toroid confirm that the accretion cannot be spherically symmetric and must occur in a circumstellar disk.
- High-angular resolution radio continuum observations and water maser emission indicate that the HC HII region is expanding on a very short time scale. The infalling gas is no longer accreting onto the star, but is stopped at the surface of the HC HII region, right at the shock front traced by the H<sub>2</sub>O maser spots.
- CH<sub>3</sub>OH masers appear to lie further from the HC HII region, may be located in the pre-shock material, and might still be participating in the infall (proper motions should be directed towards the HC HII).
- Even if the accretion phase were finished, the presence of a rotating toroid infalling on a HC HII located at the base of a powerful bipolar outflow is broadly in agreement with the expectations of the non-spherical accretion scenario for the formation of massive stars.
- Has the star reached its final mass or is the detected shell expansion an episodic process?

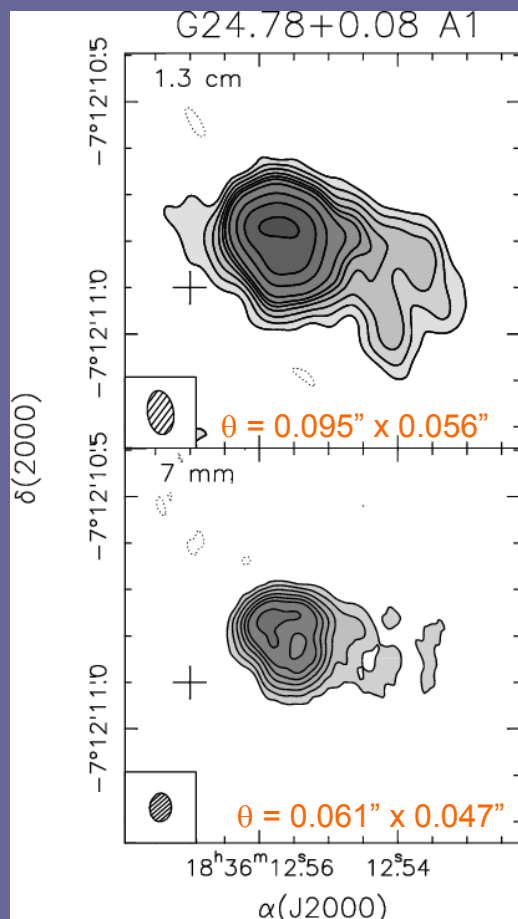




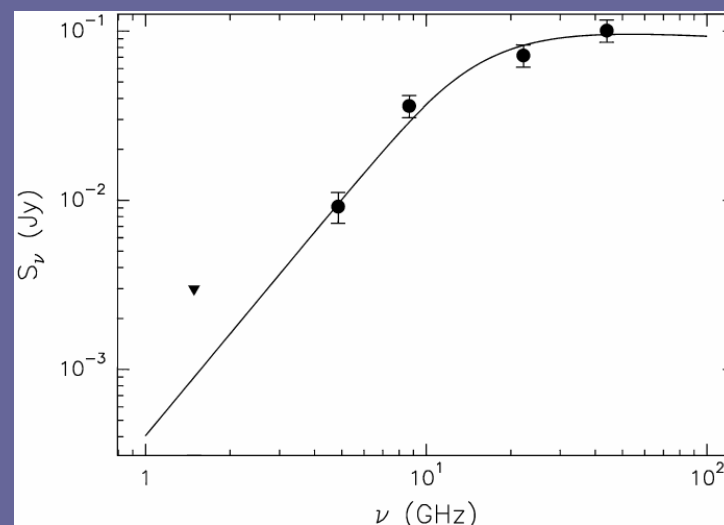
# G24.78+0.08 A1: expansion?

- The HC III region has a ring-shaped structure with an outer radius of  $\sim 590$  AU with the  $\text{H}_2\text{O}$  maser features distributed along the border of the ionized gas.

VLA + Pie Town 1.3cm and 7mm

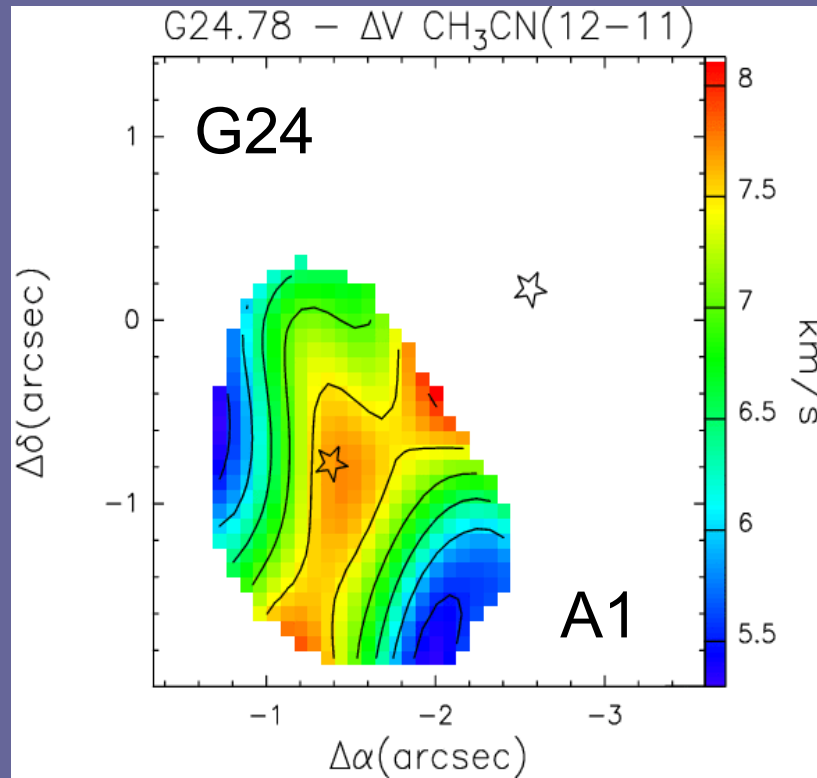


Beltrán et al. (2007)



- The radio continuum spectrum of G24 A1 and the fit obtained for a classical Strömgen HII region with a radius of  $\sim 1000$  AU and a stellar Lyman continuum of  $6.7 \times 10^{47} \text{ s}^{-1}$ , corresponding to an O9.5 type star.
- According to Shull (1980), the free-free spectrum of a shell HII region is basically indistinguishable from that of an homogeneous, spherical Strömgen HII region with the same angular radius and Lyman continuum. The only distinction between the shell and the spherical models is the presence of limb brightening at optically thin frequencies.

# G24.78+0.08 A1: linewidth

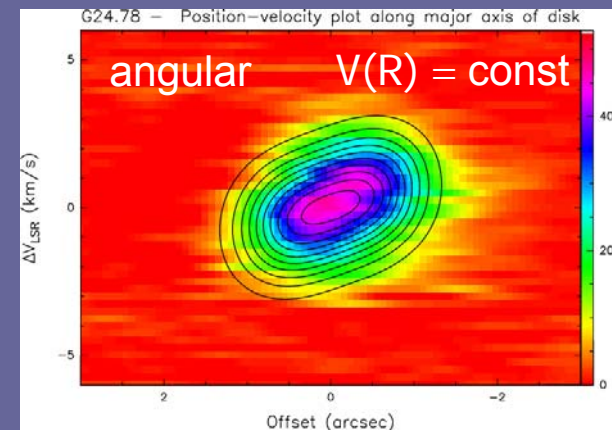
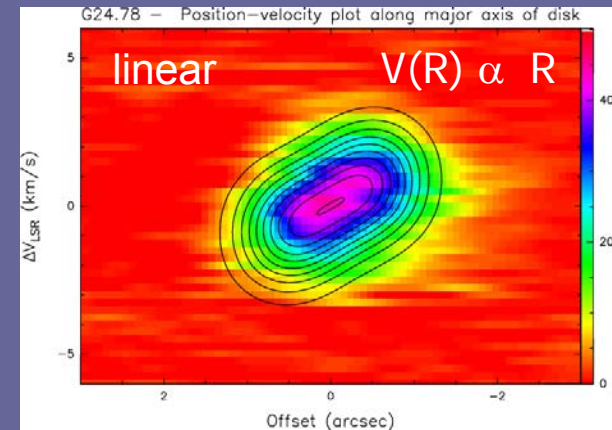
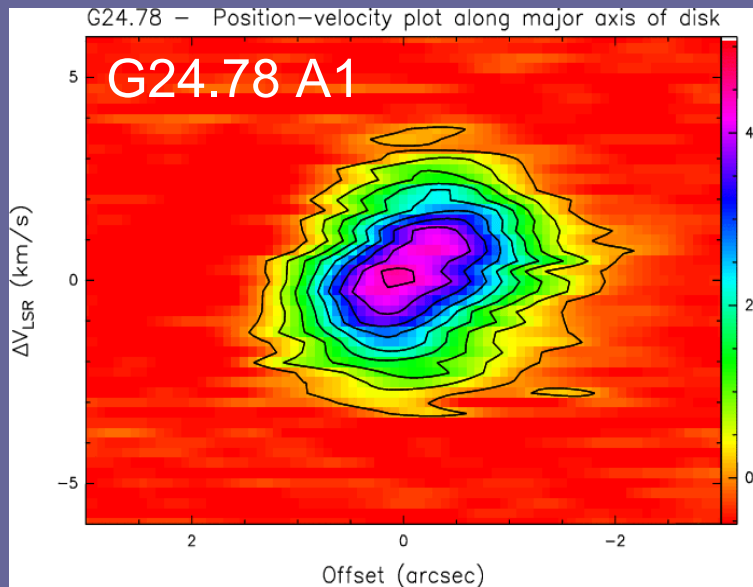


Beltrán et al. (2005)

# G24.78+0.08 A1: Modeling the velocity field (I)

- Model of CH<sub>3</sub>CN emission assuming that arises from a rotating toroid seen edge-on.
- Power-law dependence on the distance for  $v$ ,  $r$ ,  $T$ :  $v \propto R^\gamma$ ,  $\rho \propto R^{-p}$ ,  $T \propto R^{-q}$
- Radiative transfer solved for a given column density and line width
- Parameters of model:  $R_{in}$ ,  $R_{out}$ ,  $N_{CH_3CN}$ ,  $\Delta V$ ,  $p$ ,  $T_{out}$ ,  $q$ ,  $v_{rot}(R_{out})$
- NO keplerian rotation:
  - I. constant rotation velocity  $v = \text{const}$  (more unstable)
  - II. constant angular velocity  $v \propto R$  ( $B$  dominates, more equilibrium)
- Temperature gradient  $T \propto R^{-3/4}$
- Density power-law indices  $p = 1-2$

# G24.78+0.08 A1: Modeling the velocity field (II)



- With or without T gradient
- $\rho \propto R^{-1}$
- $V_{\text{rot}} \sim 2 \text{ km/s}$
- $R_{\text{inn}} \sim 2300 \text{ AU}$
- $R_{\text{out}} \sim 7700 \text{ AU}$
- $T_{\text{out}} \sim 100 \text{ K}$